

Investigating the correlation between ZTF TDEs and IceCube high-energy neutrinos

MING-XUAN LU,¹ YUN-FENG LIANG,¹ XIANG-GAO WANG,¹ AND XUE-RUI OUYANG¹

¹*Guangxi Key Laboratory for Relativistic Astrophysics, School of Physical Science and Technology, Guangxi University, Nanning 530004, China*

ABSTRACT

The main contributors of the IceCube diffuse neutrino flux remain unclear. Tidal disruption events (TDEs) have been proposed as potential emitters of the high-energy neutrinos detected by IceCube. Therefore, investigating the correlation between the TDE population and IceCube neutrinos could help us better understand whether the TDE population could be potential high-energy neutrino emitters. In this paper, we perform a systematic search for TDEs that are associated with neutrinos in a sample including 143 IceCube neutrino alert events and 61 TDEs classified by the Zwicky Transient Facility (ZTF) - Bright Transient Survey (BTS). Furthermore, considering that the TDEs/TDE candidates reported as potential IceCube neutrino emitters are all accompanied by infrared (IR) observations, we further select the TDEs with IR observations from these 61 TDEs as a subsample to examine the correlation with neutrinos. Based on the Wide-field Infrared Survey Explorer (WISE) mission database, seven TDEs are identified as having IR observations. Due to good spatial localization is crucial for association analysis, we employ two methods to handle alert events with large error radii in our sample. Then we employ three Monte Carlo simulation methods to investigate the correlation between TDE sample/subsample and IceCube neutrinos. Finally, after considering spatial and temporal criteria, seven TDEs with IR flares show the most significant correlation at a 2.43σ confidence level. If we tentatively further take the time delay factor into account in the weighting scheme, the correlation enhances to 2.54σ confidence level.

1. INTRODUCTION

The detection of the TeV-PeV diffuse astrophysical neutrino flux by IceCube (Aartsen et al. 2013a, 2014a, 2015, 2016, 2020a; Abbasi et al. 2021a, 2022a) has unveiled new possibilities for exploration in both astrophysics (Kistler & Beacom 2006; Beacom & Kistler 2007; Murase et al. 2011; Murase & Ioka 2013; Murase et al. 2013; Ahlers & Halzen 2014; Tamborra et al. 2014; Murase et al. 2014; Bechtol et al. 2017; Kistler & Laha 2018; Bartos et al. 2017; Sudoh et al. 2018; Bartos et al. 2019; Bustamante & Ahlers 2019; Hovatta et al. 2021; Ackermann et al. 2022) and particle physics (Gonzalez-Garcia et al. 2005; Ioka & Murase 2014; Ng & Beacom 2014; Aartsen et al. 2017a; Bustamante & Connolly 2019; Zhou & Beacom 2020a,b, 2022; Aartsen et al. 2021; Ackermann et al. 2022; Guo et al. 2023; Plestid & Zhou 2024; Lü et al. 2024). Despite a significant number of studies have been conducted to identify the sources of these astrophysical neutrinos. (Abbasi et al. 2011; Aartsen et al. 2013b, 2014b; Adrian-Martinez et al. 2016; Aartsen et al. 2017b,c, 2019a, 2020b, 2019b, 2020c; Lu et al. 2024; Kouch et al. 2024). It remains unclear which astrophysical sources are the principal origins of these neutrinos, although the nearby Seyfert galaxy NGC 1068 has been identified as a neutrino source at the 4.2σ confidence level (Abbasi et al. 2022b).

Among various astrophysical sources, tidal disruption events (TDEs) have been proposed as potential emitters of high-energy neutrinos. TDE is a class of bright transients, and the general picture of TDE involves a star being tidally disrupted when it approaches sufficiently close to a supermassive black hole (SMBH). A portion of the disrupted stellar debris is subsequently accreted by the SMBH, resulting in the production of an electromagnetic flare that occurs over timescales ranging from months to years (Rees 1988). Numerous models have been proposed to explain the origin of the nonthermal electromagnetic and neutrino emissions from TDEs, including relativistic jets (Wang et al. 2011;

Wang & Liu 2016; Dai & Fang 2017; Senno et al. 2017), accretion disks (Hayasaki & Yamazaki 2019), wide-angle outflows/hidden winds (Fang et al. 2020), and tidal stream interactions (Dai et al. 2015; Hayasaki & Yamazaki 2019).

Among the TDEs/TDE candidates that have been reported as potential IceCube neutrino emitters, three notable events include: one identified TDE AT2019dsg (Stein et al. 2021), and two TDE candidates, AT2019fdr (Reusch et al. 2022) and AT2019aalc (van Velzen et al. 2024), which correspond to the possibly associated alert events IC191001A, IC200530A, and IC19119A, respectively. In these three events, AT2019dsg has been classified as a member of TDE by the Zwicky Transient Facility (ZTF). The long-lived nonthermal emission detected in AT2019dsg (Cendes et al. 2021; Stein et al. 2021) suggests that mildly relativistic outflows may provide an ideal environment for neutrino production. In contrast, the classification of AT2019fdr as a TDE is somewhat uncertain, as the flare occurred in a known active galactic nucleus (AGN), complicating its origin due to the presence of an accretion disk (e.g., Trakhtenbrot et al. 2019; Frederick et al. 2021; Cendes et al. 2021). Similarly, AT2019aalc is also posited to be a flare originating from another known AGN (van Velzen et al. 2024; Veres et al. 2024). These three events share several comparable characteristics, for instance, they have bright optical luminosities, while accompanying a delayed emission in infrared (IR) observation. Further, all of these events have a time delay for the neutrino detection, which has been explained by some models (Liu et al. 2020; Murase et al. 2020; Winter & Lunardini 2021; Hayasaki 2021; Wu et al. 2022; Winter & Lunardini 2023; Mukhopadhyay et al. 2024).

Besides these three sources, there are other TDEs / TDE candidates that have also been reported as possible IceCube high-energy neutrino emitters. For instance, Jiang et al. (2023) reported two obscured TDE candidates as potential neutrino emitters based on a sample of mid-IR outbursts in nearby galaxies (MIRONG). Yuan et al. (2024) reported a super-bright TDE candidate with IR emission that satisfies spatial-temporal coincidence when considering systematic errors. Recently, Li et al. (2024) reported another TDE that is associated with a potential high-energy neutrino flare at a 2.9σ confidence level, which also accompanies IR observation.

As more and more TDEs/TDE candidates are reported as potential IceCube high-energy neutrino emitters, investigating the correlation between the TDE population and high-energy neutrinos is helpful for understanding whether the TDE population could indeed be contributors to the IceCube neutrino flux. In this work, we investigate the hypothesis that the TDE population is correlated with IceCube alert events¹. We utilize the TDEs classified by ZTF - Bright Transient Survey (BTS)² (Perley et al. 2020), which is a public catalog with a strict pipeline to conduct a classification for transient sources, and a magnitude-limited ($m < 19$ mag in either the g or r filter) survey for extragalactic transients in the ZTF public stream (Perley et al. 2020). We systematically search for spatial association events between TDEs of the ZTF-BTS catalog and IceCube alert events, while allowing a time delay between TDEs and the alert events. Since IR echoes is detected from all the TDEs/TDE candidates that are reported as potential IceCube neutrino emitters, we also systemically search for the IR emission at the coordinates of ZTF-BTS TDEs using the Wide-field Infrared Survey Explorer (WISE) mission database (Wright et al. 2010). Thus, we further adopt TDEs with IR observations as a subsample to investigate the correlation with IceCube high-energy neutrinos.

2. SAMPLE

2.1. TDE sample

The ZTF conducts a two-day cadence survey of the visible northern sky ($\sim 3\pi$) with newly found transient candidates announced via public alerts. To complement the photometric survey, the ZTF-BTS undertakes an extensive spectroscopic campaign. Since 2018 April 1, ZTF-BTS has aimed to spectroscopically classify all extragalactic transients with a magnitude of $m < 18.5$ mag (and discoveries with $m < 19$ mag) in the g or r filters, with the classifications made publicly available (Fremling et al. 2020). The survey contains thousands of objects and is updated nearly daily. This catalog offers a comprehensive and purely magnitude-limited sample of extragalactic transients, suitable for detailed statistical and demographic analysis. The ZTF-BTS catalog sets a series of stringent quality criteria to classify transients, such as magnitude limit, observation times and Galactic extinction limit (see Perley et al. (2020) for details). Therefore, this catalog could provide several TDEs that have been reliably identified for performing this correlation analysis. We select TDEs according to the classifications³ reported by ZTF-BTS, including 61 TDEs³, as shown in Fig 2.

¹ https://gcn.gsfc.nasa.gov/amon_icecube_gold_bronze_events.html

² <https://sites.astro.caltech.edu/ztf/bts/bts.php>

³ We note that AT2019fdr is classified as a supernova and AT2019aalc is not included in the ZTF-BTS catalog.

Then we search for the IR emission from coordinates of 61 ZTF-BTS TDEs using the Near-Earth Object WISE Reactivation database⁴ (NEOWISE-R; Mainzer et al. 2014; NEOWISE Team 2020). NEOWISE-R database is based on an imaging survey centered at 3.4 and 4.6 μm (labeled W1 and W2). The photometric measurements are obtained from the fitting of the point-spread function (PSF), where the PSFs are estimated from observations involving tens of thousands of stars. The NEOWISE-R magnitudes are measured through PSF fitting for individual exposures, which have been utilized to examine the IR flares for astrophysical sources (e.g., Jiang et al. 2021).

The obtained single-exposure data are initially filtered according to the quality flags indicated in the catalogs. We exclude the bad data points with poor-quality frames ($qi_fact < 1$), charged particle hits ($saa_sep < 5$), scattered moonlight ($moon_masked = 1$), and artifacts ($cc_flags \neq 0$). Additionally, data is abandoned when multiple PSF components ($nb > 1$ and $na > 0$) are present during photometry, particularly when the source is fitted concurrently with other nearby detections or when a single detection is split into two components during the fitting process. To examine the variability of IR emission at the positions of TDEs, we estimate the magnitudes by adopting the median values of the data points. Then we qualify the significance of variability in IR emission at the position of each TDE and take uncertainties into consideration, as given by Jiang et al. (2021),

$$\Delta W_{i,\sigma} = (W_{i,\max} - W_{i,\min}) / \sqrt{(W_{i,\max,\text{err}}^2 + W_{i,\min,\text{err}}^2)} \quad (1)$$

where, $W_{i,\max}$ and $W_{i,\min}$ are the maximum and minimum magnitude for i -th band, respectively. $W_{i,\max,\text{err}}$ is the error of $W_{i,\max}$ and $W_{i,\min,\text{err}}$ is the error of $W_{i,\min}$. To identify the IR flare, we impose a requirement that the IR valid variability, denoted as $\Delta W_{W1,\sigma}$ or $\Delta W_{W2,\sigma}$, must exceed 5σ . Meanwhile, the IR flares should only occur after the discovery dates of TDEs, where the discovery dates of TDEs are obtained from Transient Name Server (TNS)⁵.

Moreover, we note that the discovery dates of five TDEs occur after the final data point of the NEOWISE-R database, namely AT2023wdb, AT2024bgz, AT2024pvu, AT2024tvd and AT2024yqo. For these five TDEs, we search for their information from Extragalactic Database (NASA/IPAC Extragalactic Database (NED) 2019), and find no report indicating that they accompany IR flares. Finally, there are seven ZTF-BTS TDEs with IR flares, as listed in Table 1. The light curves of these seven TDEs are presented in Fig 1, where red and blue circles are the W1 and W2 band data, respectively. The red dashed lines are the discovery dates of TDEs.

Table 1. ZTF-BTS TDEs with IR flares.

TNS _{ID}	Discovery date ^a	MJD	$\Delta W_{W1,\sigma}^b$	$\Delta W_{W2,\sigma}^b$
		(days)		
AT2019azh	19/02/22	58535	5.15	3.48
AT2019dsg	19/04/09	58582	18.59	16.40
AT2019qiz	19/09/19	58745	38.87	41.78
AT2020nov	20/06/27	59027	12.95	9.30
AT2022dyt	22/02/26	59635	7.96	7.37
AT2022upj	22/08/31	59822	30.36	16.17
AT2023cvb	23/03/06	60009	7.76	6.77

^a The discovery dates of TDEs obtained from TNS.

^b The significance of the IR variability in the W1 and W2 bands.

2.2. Neutrino sample

The IceCube Neutrino Observatory has observed high-energy astrophysical neutrinos exceeding the atmospheric background in both cascade and track data. Since 2016, real-time alerts for individual high-energy events (>100 TeV) have been released to the multimessenger observational community through platforms, for example, the Global Cycling Network (GCN)⁶. These alert events concentrate on track-like neutrino candidates, which provide more precise angular localizations compared to cascade events. Since June 2019, all alert events have been assigned a signalness value and

⁴ https://irsa.ipac.caltech.edu/cgi-bin/Gator/nph-dd?catalog=neowiser_p1bs_psd

⁵ <https://www.wis-tns.org/search>

⁶ <https://gcn.nasa.gov/circulars?query=IceCube&startDate=&endDate=&sort=circularID&limit=100>

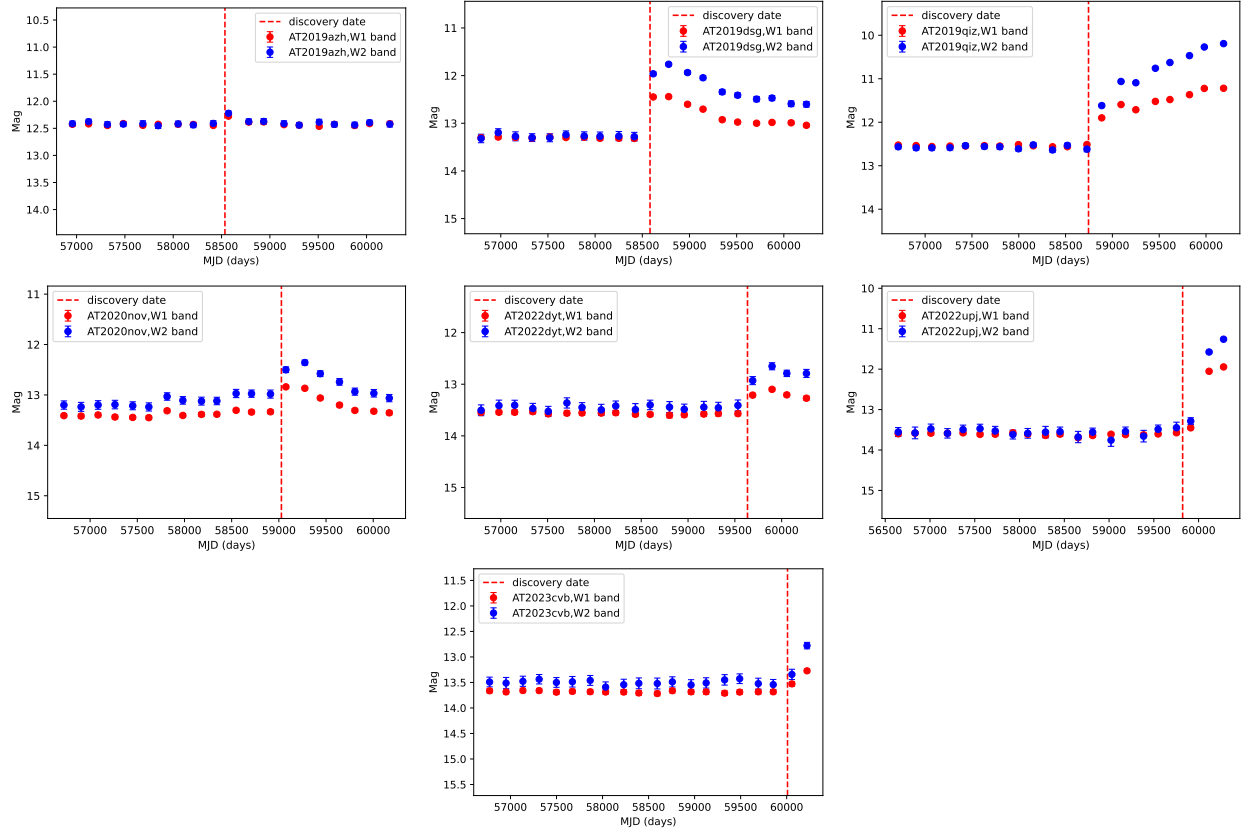


Figure 1. The IR light curves of seven ZTF-BTS TDEs with $> 5\sigma$ IR flares, where the red and blue points represent the W1 and W2 band data, respectively. The vertical line denotes the discovery date of the TDE.

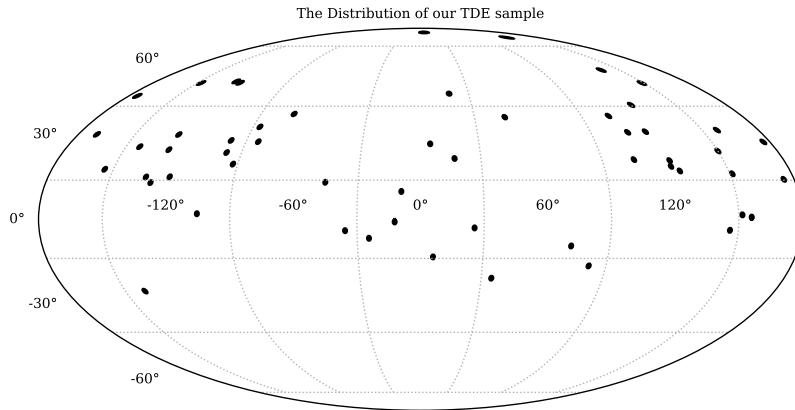


Figure 2. The sky distribution in celestial coordinates of the 61 ZTF-BTS TDEs considered in this work.

categorized as either gold or bronze based on their probability of astrophysical origin, specifically larger than 50% and 30%, respectively. The 90% containment error radius (r_{90} ⁷) for these alert events are publicly available. For each alert event, an updated report would be provided after detecting a more accurate position. The latest reported information for each alert event is adopted in our analysis, while we note that one alert event⁸ (i.e. IC241016) is found to clearly not be of astrophysical origin so that we remove it from our sample. We also note that Abbasi et al. (2023a) has

⁷ Noting that the r_{90} only contains statistical error as described in https://gcn.gsfc.nasa.gov/amon_icecube_gold_bronze_events.html

⁸ <https://gcn.nasa.gov/circulars/37794?query=IceCube&startDate=&endDate=&sort=circularID&limit=100>

provided updated r_{90} for neutrinos between 2011 and 2020. However, compared to the catalog covering the period from 2011 to 2020, our primary focus is on the neutrinos published after 2019, as this period suitably matches the ZTF-BTS catalog survey timeline i.e. allowing for alert events occur after the TDEs of ZTF-BTS catalog. Therefore, for our analysis, we adopt the list of all the bronze and gold alert events after 2019 as our sample, leaving at least a 30% probability of an astrophysical origin for these alert events.

Furthermore, for the association analysis, it is crucial that neutrino events have a good spatial localization. Some studies exclude alert events if their 90% confidence level error region area, denoted as Ω_{90} , exceeds a threshold value (e.g., [Plavin et al. \(2020\)](#); [Hovatta et al. \(2021\)](#)). More recently, rather than directly excluding alert events, [Kouch et al. \(2024\)](#) proposed a weighting scheme that gradually reduces the effect of alert events with large error regions in the association analysis. The weighting scheme removes the need for setting arbitrary selection thresholds and takes into account observed information, including the signalness and Ω_{90} of alert events in the correlation analysis.

Therefore, in this analysis, we employ two methods to handle our alert events sample. The first method involves noting that AT 2019dsg associates with an alert event of $\Omega_{90} \sim 30 \text{ deg}^2$ so that we exclude alert events of Ω_{90} larger than 30 deg^2 . The other method combines the information of signalness and Ω_{90} using the weighting scheme to perform this correlation analysis.

3. ANALYSIS METHOD

We perform a systematic search in our samples based on the spatial and temporal criteria. The initial step involves examining the spatial correlation between TDEs and alert events. This is realized by cross-correlating the coordinates of TDEs within r_{90} of the alert events. In this step, we search for spatially associated events, using the alert events sample with $\Omega_{90} < 30 \text{ deg}^2$ and the whole alert events sample, respectively. According to the r_{90} of IceCube alert events, the calculation of Ω_{90} for alert events is given by [Kouch et al. \(2024\)](#),

$$\Omega = \frac{\pi}{4}(\text{RA}^+ \times \text{DEC}^+ + \text{RA}^- \times \text{DEC}^+ + \text{RA}^+ \times \text{DEC}^- + \text{RA}^- \times \text{DEC}^-) \quad (2)$$

where, $\text{RA}^+, \text{RA}^-, \text{DEC}^+$ and DEC^- are the four directional errors, respectively. In this case, we employ the r_{90} of alert events in these four directions.

In the next step, we identify the temporal coincident events from the spatially correlated events, i.e., these TDEs that were discovered before the arrival dates of alert events. Therefore, the test-statistic (TS) parameter is the time delay (ΔT , the arrival date of the alert event subtracting the discovery date of TDE). If one TDE is found within the r_{90} of an alert event and $\Delta T > 0$, the TS value would be increased by 1. During the calculation of TS values, we allow that a single TDE or alert event can contribute repeatedly to the TS values. Specifically, if one alert event is spatially and temporally associated with N TDEs, or if one TDE is spatially and temporally associated with N alert events, they can each contribute a TS value of N (i.e., the total TS will be plus N).

As mentioned above, we consider two methods to handle the sample of alert events. The first method involves excluding alert events of $\Omega_{90} > 30 \text{ deg}^2$ (hereafter referred to CUT method). In this scenario, the number of TDEs that are spatially-temporally associated with the alert events corresponds to the TS values.

The other method includes the whole alert events sample while assigning a weight factor that combines the Ω_{90} and signalness of alert events (hereafter referred to WEIGHT method). The weighting factor can be expressed as ([Kouch et al. 2024](#)),

$$\mathcal{W}_i = \begin{cases} S_i & \text{for } \Omega_{90,i} \leq M(\Omega_{90}) \\ S_i \times \frac{M(\Omega_{90})}{\Omega_{90,i}} & \text{for } \Omega_{90,i} > M(\Omega_{90}) \end{cases} \quad (3a)$$

$$(3b)$$

where, S_i and $\Omega_{90,i}$ are the signalness and Ω_{90} for the i -th alert event, respectively. $M(\Omega_{90})$ is the median of Ω_{90} of alert events sample. In the weighting scheme, the weight factor is implemented in the calculation of TS values by multiplying \mathcal{W}_i when TDEs are found to be spatially-temporally associated with the i -th alert event.

According to the r_{90} of the alert events and Eq. 2, we estimate that the $M(\Omega_{90})$ of our alert events sample is 6.88 deg^2 . We present the TS values using the heating map after considering the weight factor, as shown in Fig 3, where the color bar is the TS value when one TDE is found to be associated with an alert event, the black dashed line indicates the median value of our alert events sample (6.88 deg^2), inverted triangles are alert events that are not associated any TDE and the red stars present alert events that are spatially-temporally associated with at least one

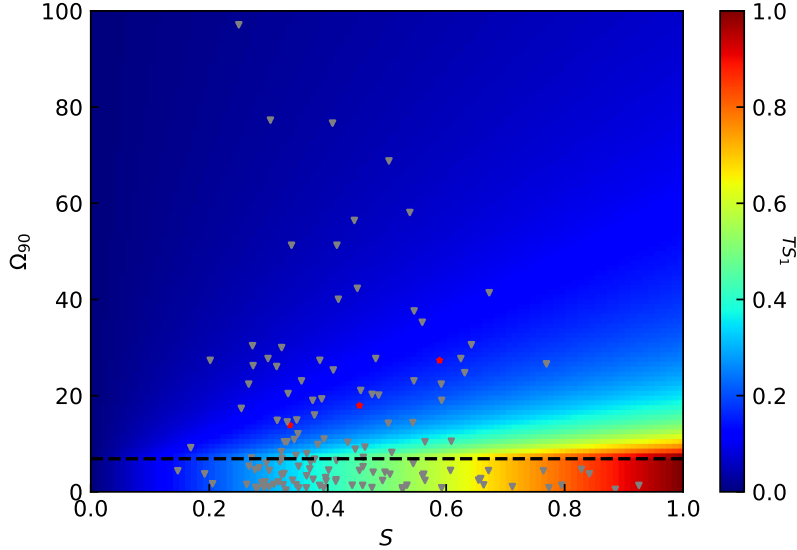


Figure 3. This plot shows the distribution of the IceCube alert events in the $\Omega_{90} - S$ plane, where Ω_{90} is the event’s error region size and S is the signalness. The red stars represent the alert events that are spatially associated with at least one TDE (i.e., the TDE is within the error region of the event), while the inverted triangles are alert events that are not associated with any TDE. The black dashed line indicates the median Ω_{90} value (6.88 deg^2) of our alert events sample. This plot only includes alert events where $\Omega_{90} < 100 \text{ deg}^2$. The color map shows the 1-event TS value (TS_1) that an alert event could contribute to the total TS value in the WEIGHT method of the correlation analysis, which depends on the Ω_{90} and S of the alert event.

TDE, respectively. One can see that the Ω_{90} values of alert events that are associated with TDEs are larger than the median value.

Based on these two methods for handling the alert events sample, three MC simulation methods are adopted to perform a correlation analysis between the TDEs population and the alert events population. They are described as follows.

Method I: similar to previous works (e.g., Plavin et al. 2020; Hovatta et al. 2021), due to the sensitivity of IceCube only depends on the zenith angle (Aartsen et al. 2017d), we only randomize the RA of the alert events, while keeping the DEC fixed. The r_{90} and arrival date are consistent with their observed one for each alert event, and the information about the TDEs remains fixed.

Method II: we not only randomize the RA of alert events, as in Method I, but also simulate the TDE sample using the method described in Lu et al. (2024). The method for simulating the TDE sample is as follows. We randomly select RA' and DEC' from the observed lists of RA and DEC, respectively, to represent a mock source. Furthermore, we impose an additional random shift to (RA', DEC') within a region of 10° radius. For each source, we ensure that it remains within the same sky region as the ZTF-BTS sample, which covers the northern sky with a DEC range from -30° to 90° , while excluding the Galactic plane region ($|b| < 7^\circ$). When we obtain the number of mock sources as the same as the observed one, we use the KS test to ensure that the mock sources preserve the distribution pattern of the actual sources, i.e., RA' and DEC' of mock sources are performed KS test, respectively.

Method III: the same as Method II, we also randomize the RA of alert events and TDE positions. The method used to simulate the TDE sample is consistent with Buson et al. (2022, 2023); Bellenghi et al. (2023). We simulate TDEs by randomizing the positions of the sources within a 10° -radius range from their original positions. During this process, we also ensure that each pseudo-source remains within the sky region of the ZTF-BTS sample. The KS test is also performed in the same manner as in Method II.

By realizing 10^4 times MC simulations to obtain the TS distribution. We can then estimate the chance probability (i.e., the p value of rejecting the null hypothesis) by counting the fraction of TS values that are equal to or larger than the observed value,

$$p = \frac{M + 1}{N + 1} \quad (4)$$

where M is the number of TS values equal to or larger than the observed one and N is the total number of MC simulations (Davison & Hinkley 1997). Then, we can estimate the p values for these three MC simulation methods.

4. RESULTS

We first systematically search for associated events that satisfy spatial and temporal criteria. After adopting the CUT method, there are 122 alert events remaining in our sample. Three associated events are found, and two of these events have IR flares, which are listed in Table 2. Apart from AT2019dsg, two other TDEs are associated with two bronze alert events.

Under the WEIGHT method, all 143 alert events are utilized to search for associated events. We found that there are seven occurrences of TDEs within the r_{90} of five alert events. Among them, one TDE (AT2019azh) is located within r_{90} of two alert events. Additionally, the r_{90} of two alert events each includes two TDEs. However, we note that the r_{90} values of these two alert events are significantly large ($> 10^\circ$), contributing only negligible TS values. In total, six distinct TDEs are found within r_{90} of five alert events, two of which have IR flares, as listed in Table 3.

Table 2. Associated events when excluding alert events with error regions larger than 30 deg^2 .

RA _{alert}	DEC _{alert}	r_{90}	T_{alert}	Signalness	TDE event	ΔT^a	TS ₁ value ^b	IR flare ^c
(deg)	(deg)	(deg)				(days)		
124.54	20.74	2.39	23/02/17	0.454	AT2019azh	1456	1	Yes
47.20	-3.28	2.1	22/05/24	0.336	AT2020afhd	581	1	No
314.08	12.94	2.95	19/10/01	0.589	AT2019dsg	175	1	Yes

^a The time delay between the alert event arrival date T_{alert} and the TDE discovery date.

^b In the CUT method, each association contributes $TS = 1$ to the total TS value of the correlation.

^c This column indicates whether the TDEs have IR flares.

Table 3. Associated events considering the whole alert sample in the WEIGHT method.

RA _{alert}	DEC _{alert}	r_{90}	Date _{alert}	Signalness	TDE event	ΔT^a	TS ₁ value ^b	IR flare ^c
(deg)	(deg)	(deg)				(days)		
239.63	39.94	15.38	24/03/07	0.606	AT2020vwl	1244	0.0056	No
239.63	39.94	15.38	24/03/07	0.606	AT2020pj	1526	0.0056	No
127.18	20.74	10.16	23/07/07	0.466	AT2022bdw	522	0.010	No
127.18	20.74	10.16	23/07/07	0.466	AT2019azh	1596	0.010	Yes
124.54	20.74	2.39	23/02/17	0.454	AT2019azh	1456	0.17	Yes
47.20	-3.28	2.1	22/05/24	0.336	AT2020afhd	581	0.17	No
314.08	12.94	2.95	19/10/01	0.589	AT2019dsg	175	0.15	Yes

^a The time delay between the alert event arrival date T_{alert} and the TDE discovery date.

^b The 1-event TS represents the value that an association event can contribute to the total TS of the correlation.

^c This column indicates whether the TDEs have IR flares.

We employ three MC simulation methods, as described in Sec. 3, to estimate the p values for these search results. Each estimation is performed using 10^4 times MC simulations. For instance, if using the all TDEs sample and simulating Method III, the TS distribution obtained from 10^4 times MC simulations is shown in Fig 4, where the left panel illustrates the TS distribution when the CUT method is applied, and the right panel corresponds to the WEIGHT method. The blue region represents the simulated TS distribution, while the red dashed line indicates the observed TS value. The region to the right of the red dashed line corresponds to simulated TS values that are equal to or greater than the observed TS value.

By realizing 10^4 times MC simulations, the results obtained from the three MC methods are summarized in Table 4, which includes the results from both the CUT method and the WEIGHT method. Using the all TDEs sample, the best p -values are 0.15 and 0.32 for the CUT method and WEIGHT method, respectively. When using the subsample of TDEs with IR flares, the best p -values are 0.015 and 0.044 for the CUT method and WEIGHT method, corresponding to 2.43σ and 2.01σ , respectively. The most significant correlation with neutrinos is obtained from the subsample of

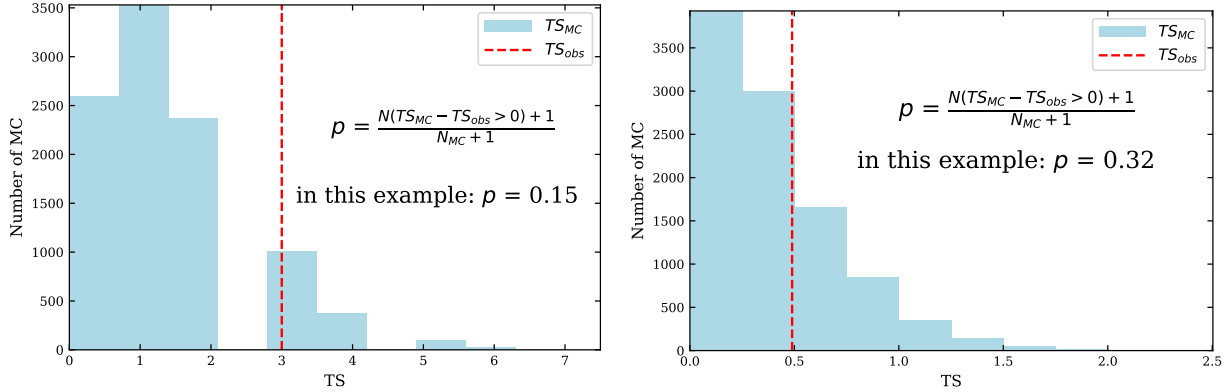


Figure 4. The example (MC method III+All TDEs) for TS distribution obtained from 10^4 MC simulations, where the left panel and right panel are the TS distribution using CUT and WEIGHT methods, respectively.

Table 4. The p -values of the TDE-neutrino correlation obtained in different MC methods.

	Method I	Method II	Method III	TDE sample ^a
CUT method	0.16	0.15	0.15	All TDEs
WEIGHT method	0.34	0.32	0.32	All TDEs
CUT method	0.027	0.015	0.020	TDEs with IR flare
WEIGHT method	0.044	0.044	0.047	TDEs with IR flare

TDEs with IR flare at a $\sim 2.43\sigma$ confidence level, which may indicate that TDEs with IR flare are more likely to correlate with IceCube neutrinos compared to all TDEs sample.

5. DISCUSSION

5.1. The systematic errors of alert events

Although the IceCube collaboration strives to consider all potential errors in estimating the size of the high-energy neutrino error regions, there may still be some unknown systematic errors, such as those arising from ice inhomogeneities, that cannot be completely addressed (e.g. Abbasi et al. 2023b). An upper limit of 1° is estimated for this systematic error by Aartsen et al. (2013c). While efforts to constrain this parameter are ongoing (Abbasi et al. 2021b, 2022c), the most recent findings suggest that the associated error is likely negligible (Abbasi et al. 2022c, 2023b).

In this work, we add a systematic error upper limit of 1° in quadrature to the four directions of RA and DEC, so that the final uncertainty in each direction is $\sqrt{r_{90}^2 + (1^\circ)^2}$. We then search for associated events among all alert events (having added 1° systematic error) and TDEs. However, no additional associated events are found when compared to those listed in Table 3. Therefore, the p value is expected to increase as the systematic error grows larger within the range of $0^\circ \sim 1^\circ$. When a 1° systematic error is added to each alert event, the $M(\Omega_{90})$ of the alert events sample is 10.02 deg^2 . We only adopt the WEIGHT method to perform the effect of systemic error on the estimation of p values. The p values estimated by three MC simulation methods are listed in Table 5, showing an increase of $\sim 20\%$ to $\sim 45\%$ compared to those in Table 4.

Table 5. p -value results when introducing 1° systematic error or time delay factor.

	Method I	Method II	Method III	TDE sample ^a
WEIGHT+Syst.	0.44	0.45	0.43	All TDEs
WEIGHT+Syst.	0.060	0.054	0.068	TDEs with IR flare
WEIGHT+Delay	0.29	0.30	0.28	All TDEs
WEIGHT+Delay	0.011	0.043	0.032	TDEs with IR flare

5.2. Time delay factor

In this analysis, the temporal coincidence criterion is required that the discovery dates of TDEs are earlier than the arrival dates of alert events. In this scenario, we estimate the p values of correlation between TDEs/subsample of ZTF-BTS catalog and IceCube neutrinos, and the most significant correlation is given by the TDEs with IR flares subsample.

However, observationally, the time delays of potentially associated events between TDEs/TDE candidates and IceCube neutrinos are reported to range from several months to years. For instance, one bona fide TDE, AT2019dsg shows a time delay of \sim half a year. The other two TDE candidates i.e. AT2019fdr and AT2019aalc show a time delay of \sim half a year and \sim one year after the discovery dates of TDE candidates, respectively. AT2021lwx also presents a time delay of \sim one year. Although the accurate time delay still remains obscure due to the limited number of potentially associated events reported so far, these events present a time delay within a span of \sim one year.

Therefore, we tentatively impose a time delay factor into the weighting scheme to reduce the weight of associated events with large time delays. By combining an additional time delay factor into the weight factor of Eq. 3a, 3b, we reduce the impact of events with large time delays, i.e.

$$\mathcal{W}_i = \begin{cases} S_i/\Delta T & \text{for } \Omega_{90,i} \leq M(\Omega_{90}) \\ S_i/\Delta T \times \frac{M(\Omega_{90})}{\Omega_{90,i}} & \text{for } \Omega_{90,i} > M(\Omega_{90}) \end{cases} \quad (5a)$$

After adding the time delay factor, the TS values are mainly contributed by the AT2019dsg event. By realizing 10^4 times MC simulations, the p values for the three MC simulation methods are summarized in Table 5. Compared to the results without the time delay factor, the best p value of the all-TDEs sample decreases to 0.28, while that for the TDEs with IR flares subsample decreases to 0.011 ($\sim 2.54\sigma$). After introducing the time delay factor, the subsample with IR flare also presents the most significant correlation with IceCube neutrinos compared to the all-TDEs sample.

6. SUMMARY

Currently, the main contributors to the IceCube neutrino flux are still obscure. Among various astrophysical sources, TDEs have been suggested as possible emitters of IceCube neutrinos. Therefore, investigating the correlation between the TDE population and IceCube neutrinos could help us better understand whether TDEs could really serve as neutrino emitters. In this work, we study the correlation between the TDEs/TDE candidates from the ZTF-BTS catalog and the population of IceCube neutrinos. Considering that good spatial localization is crucial for establishing reliable association, we employ two methods to handle the alert events with large error circles. One method involves directly excluding alert events with error area $\Omega_{90} > 30 \text{ deg}^2$, while another method introduces a weighting factor. We quantify the significance of the correlation using three MC simulation methods. By performing MC simulations, we find that the subsample of TDEs with IR flares presents the most significant correlation with IceCube neutrinos, though still below the 3σ confidence level. We also discuss the case that includes a systematic error in the events' error radii. Given that only the statistical error is publicly available for alert events, we add a systematic error of 1° , which is the upper limit of the systematic error estimated by Aartsen et al. (2013c), in quadrature to the statistical error. There are no additional associated events arising from the inclusion of 1° systematic error and the obtained results could be treated as the upper limits of the p values. Furthermore, for the potentially associated events reported so far, the arrival dates of neutrinos are within an interval of ~ 1 year after the discovery dates of the TDEs/TDE candidates. Therefore, we tentatively introduce a time delay (ΔT) term into the weighting factor in our MC simulation to reduce the weight of large time-delayed events. By combining the time delay factor, the best p values decrease to 0.28 and 0.011 ($\sim 2.54\sigma$) for the all-TDE sample and the subsample with IR flares, respectively. However, the lowest p value remains below the 3σ confidence level, even though trial factors have not been taken into account yet. In total, at present no significant correlation is found in the population analysis between the ZTF-BTS TDEs and IceCube alert neutrino events. Our work is the first research to quantify the p -value of the TDE-neutrino association with actual TDE and neutrino observations.

ACKNOWLEDGEMENTS

This work is supported by the National Key Research and Development Program of China (Grant No. 2022YFF0503304), the National Natural Science Foundation of China (12373042, U1938201), the Programme of Bagui Scholars Programme (WXG) and Innovation Project of Guangxi Graduate Education (YCBZ2024060).

REFERENCES

- Aartsen, M. G., et al. 2013a, *Science*, 342, 1242856, doi: [10.1126/science.1242856](https://doi.org/10.1126/science.1242856)
- . 2013b, *Astrophys. J.*, 779, 132, doi: [10.1088/0004-637X/779/2/132](https://doi.org/10.1088/0004-637X/779/2/132)
- . 2013c, *Phys. Rev. Lett.*, 111, 021103, doi: [10.1103/PhysRevLett.111.021103](https://doi.org/10.1103/PhysRevLett.111.021103)
- . 2014a, *Phys. Rev. Lett.*, 113, 101101, doi: [10.1103/PhysRevLett.113.101101](https://doi.org/10.1103/PhysRevLett.113.101101)
- . 2014b, *Astrophys. J.*, 796, 109, doi: [10.1088/0004-637X/796/2/109](https://doi.org/10.1088/0004-637X/796/2/109)
- . 2015, *Astrophys. J.*, 809, 98, doi: [10.1088/0004-637X/809/1/98](https://doi.org/10.1088/0004-637X/809/1/98)
- . 2016, *Astrophys. J.*, 833, 3, doi: [10.3847/0004-637X/833/1/3](https://doi.org/10.3847/0004-637X/833/1/3)
- . 2017a, *Nature*, 551, 596, doi: [10.1038/nature24459](https://doi.org/10.1038/nature24459)
- . 2017b, *Astrophys. J.*, 835, 151, doi: [10.3847/1538-4357/835/2/151](https://doi.org/10.3847/1538-4357/835/2/151)
- . 2017c, *Astrophys. J.*, 846, 136, doi: [10.3847/1538-4357/aa8508](https://doi.org/10.3847/1538-4357/aa8508)
- . 2017d, *Astrophys. J.*, 835, 151, doi: [10.3847/1538-4357/835/2/151](https://doi.org/10.3847/1538-4357/835/2/151)
- . 2019a, *Eur. Phys. J. C*, 79, 234, doi: [10.1140/epjc/s10052-019-6680-0](https://doi.org/10.1140/epjc/s10052-019-6680-0)
- . 2019b, *Astrophys. J.*, 886, 12, doi: [10.3847/1538-4357/ab4ae2](https://doi.org/10.3847/1538-4357/ab4ae2)
- . 2020a, *Phys. Rev. Lett.*, 125, 121104, doi: [10.1103/PhysRevLett.125.121104](https://doi.org/10.1103/PhysRevLett.125.121104)
- . 2020b, *Phys. Rev. Lett.*, 124, 051103, doi: [10.1103/PhysRevLett.124.051103](https://doi.org/10.1103/PhysRevLett.124.051103)
- . 2020c, *Astrophys. J.*, 898, 117, doi: [10.3847/1538-4357/ab9fa0](https://doi.org/10.3847/1538-4357/ab9fa0)
- . 2021, *Nature*, 591, 220, doi: [10.1038/s41586-021-03256-1](https://doi.org/10.1038/s41586-021-03256-1)
- Abbasi, R., et al. 2011, *Astrophys. J.*, 732, 18, doi: [10.1088/0004-637X/732/1/18](https://doi.org/10.1088/0004-637X/732/1/18)
- . 2021a, *Phys. Rev. D*, 104, 022002, doi: [10.1103/PhysRevD.104.022002](https://doi.org/10.1103/PhysRevD.104.022002)
- . 2021b, *JINST*, 16, P07041, doi: [10.1088/1748-0221/16/07/P07041](https://doi.org/10.1088/1748-0221/16/07/P07041)
- . 2022a, *Astrophys. J.*, 928, 50, doi: [10.3847/1538-4357/ac4d29](https://doi.org/10.3847/1538-4357/ac4d29)
- . 2022b, *Science*, 378, 538, doi: [10.1126/science.abg3395](https://doi.org/10.1126/science.abg3395)
- . 2022c, *Science*, 378, 538, doi: [10.1126/science.abg3395](https://doi.org/10.1126/science.abg3395)
- . 2023a, *Astrophys. J. Suppl.*, 269, 25, doi: [10.3847/1538-4365/acfa95](https://doi.org/10.3847/1538-4365/acfa95)
- . 2023b, *Astrophys. J.*, 954, 75, doi: [10.3847/1538-4357/acdfcb](https://doi.org/10.3847/1538-4357/acdfcb)
- Ackermann, M., et al. 2022, *JHEAp*, 36, 55, doi: [10.1016/j.jheap.2022.08.001](https://doi.org/10.1016/j.jheap.2022.08.001)
- Adrian-Martinez, S., et al. 2016, *Astrophys. J.*, 823, 65, doi: [10.3847/0004-637X/823/1/65](https://doi.org/10.3847/0004-637X/823/1/65)
- Ahlers, M., & Halzen, F. 2014, *Phys. Rev. D*, 90, 043005, doi: [10.1103/PhysRevD.90.043005](https://doi.org/10.1103/PhysRevD.90.043005)
- Bartos, I., Ahrens, M., Finley, C., & Marka, S. 2017, *Phys. Rev. D*, 96, 023003, doi: [10.1103/PhysRevD.96.023003](https://doi.org/10.1103/PhysRevD.96.023003)
- Bartos, I., Veske, D., Keivani, A., et al. 2019, *Phys. Rev. D*, 100, 083017, doi: [10.1103/PhysRevD.100.083017](https://doi.org/10.1103/PhysRevD.100.083017)
- Beacom, J. F., & Kistler, M. D. 2007, *Phys. Rev. D*, 75, 083001, doi: [10.1103/PhysRevD.75.083001](https://doi.org/10.1103/PhysRevD.75.083001)
- Bechtol, K., Ahlers, M., Di Mauro, M., Ajello, M., & Vandenbroucke, J. 2017, *Astrophys. J.*, 836, 47, doi: [10.3847/1538-4357/836/1/47](https://doi.org/10.3847/1538-4357/836/1/47)
- Bellenghi, C., Padovani, P., Resconi, E., & Giommi, P. 2023, *Astrophys. J. Lett.*, 955, L32, doi: [10.3847/2041-8213/acf711](https://doi.org/10.3847/2041-8213/acf711)
- Buson, S., et al. 2022, *Astrophys. J. Lett.*, 933, L43, doi: [10.3847/2041-8213/ac7d5b](https://doi.org/10.3847/2041-8213/ac7d5b)
- Buson, S., Tramacere, A., Oswald, L., et al. 2023. <https://arxiv.org/abs/2305.11263>
- Bustamante, M., & Ahlers, M. 2019, *Phys. Rev. Lett.*, 122, 241101, doi: [10.1103/PhysRevLett.122.241101](https://doi.org/10.1103/PhysRevLett.122.241101)
- Bustamante, M., & Connolly, A. 2019, *Phys. Rev. Lett.*, 122, 041101, doi: [10.1103/PhysRevLett.122.041101](https://doi.org/10.1103/PhysRevLett.122.041101)
- Cendes, Y., Alexander, K. D., Berger, E., et al. 2021, *Astrophys. J.*, 919, 127, doi: [10.3847/1538-4357/ac110a](https://doi.org/10.3847/1538-4357/ac110a)
- Dai, L., & Fang, K. 2017, *Mon. Not. Roy. Astron. Soc.*, 469, 1354, doi: [10.1093/mnras/stx863](https://doi.org/10.1093/mnras/stx863)
- Dai, L., McKinney, J. C., & Miller, M. C. 2015, *Astrophys. J. Lett.*, 812, L39, doi: [10.1088/2041-8205/812/2/L39](https://doi.org/10.1088/2041-8205/812/2/L39)
- Davison, A. C., & Hinkley, D. V. 1997, *Bootstrap Methods and their Application*, Cambridge Series in Statistical and Probabilistic Mathematics (Cambridge University Press)
- Fang, K., Metzger, B. D., Vurm, I., Aydi, E., & Chomiuk, L. 2020, *Astrophys. J.*, 904, 4, doi: [10.3847/1538-4357/abbc6e](https://doi.org/10.3847/1538-4357/abbc6e)
- Frederick, S., et al. 2021, *Astrophys. J.*, 920, 56, doi: [10.3847/1538-4357/ac110f](https://doi.org/10.3847/1538-4357/ac110f)
- Fremling, U. C., et al. 2020, *Astrophys. J.*, 895, 32, doi: [10.3847/1538-4357/ab8943](https://doi.org/10.3847/1538-4357/ab8943)

- Gonzalez-Garcia, M. C., Halzen, F., & Maltoni, M. 2005, *Phys. Rev. D*, 71, 093010, doi: [10.1103/PhysRevD.71.093010](https://doi.org/10.1103/PhysRevD.71.093010)
- Guo, X.-K., Lü, Y.-F., Huang, Y.-B., et al. 2023, *Phys. Rev. D*, 108, 043001, doi: [10.1103/PhysRevD.108.043001](https://doi.org/10.1103/PhysRevD.108.043001)
- Hayasaki, K. 2021, doi: [10.1038/s41550-021-01309-z](https://doi.org/10.1038/s41550-021-01309-z)
- Hayasaki, K., & Yamazaki, R. 2019, doi: [10.3847/1538-4357/ab44ca](https://doi.org/10.3847/1538-4357/ab44ca)
- Hovatta, T., et al. 2021, *Astron. Astrophys.*, 650, A83, doi: [10.1051/0004-6361/202039481](https://doi.org/10.1051/0004-6361/202039481)
- Ioka, K., & Murase, K. 2014, *PTEP*, 2014, 061E01, doi: [10.1093/ptep/ptu090](https://doi.org/10.1093/ptep/ptu090)
- Jiang, N., Zhou, Z., Zhu, J., Wang, Y., & Wang, T. 2023, *Astrophys. J. Lett.*, 953, L12, doi: [10.3847/2041-8213/acebe3](https://doi.org/10.3847/2041-8213/acebe3)
- Jiang, N., Wang, T., Dou, L., et al. 2021, *ApJS*, 252, 32, doi: [10.3847/1538-4365/abd1dc](https://doi.org/10.3847/1538-4365/abd1dc)
- Kistler, M. D., & Beacom, J. F. 2006, *Phys. Rev. D*, 74, 063007, doi: [10.1103/PhysRevD.74.063007](https://doi.org/10.1103/PhysRevD.74.063007)
- Kistler, M. D., & Laha, R. 2018, *Phys. Rev. Lett.*, 120, 241105, doi: [10.1103/PhysRevLett.120.241105](https://doi.org/10.1103/PhysRevLett.120.241105)
- Kouch, P. M., et al. 2024, *Astron. Astrophys.*, 690, A111, doi: [10.1051/0004-6361/202347624](https://doi.org/10.1051/0004-6361/202347624)
- Li, R.-L., Yuan, C., He, H.-N., et al. 2024, <https://arxiv.org/abs/2411.06440>
- Liu, R.-Y., Xi, S.-Q., & Wang, X.-Y. 2020, *Phys. Rev. D*, 102, 083028, doi: [10.1103/PhysRevD.102.083028](https://doi.org/10.1103/PhysRevD.102.083028)
- Lu, M.-X., Liang, Y.-F., Ouyang, X., Li, R.-L., & Wang, X.-G. 2024, <https://arxiv.org/abs/2404.19730>
- Lü, Y.-F., Zhu, B.-Y., Li, R.-L., et al. 2024, *Res. Astron. Astrophys.*, 24, 035008, doi: [10.1088/1674-4527/ad204e](https://doi.org/10.1088/1674-4527/ad204e)
- Mainzer, A., Bauer, J., Cutri, R. M., et al. 2014, *ApJ*, 792, 30, doi: [10.1088/0004-637X/792/1/30](https://doi.org/10.1088/0004-637X/792/1/30)
- Mukhopadhyay, M., Bhattacharya, M., & Murase, K. 2024, *Mon. Not. Roy. Astron. Soc.*, 534, 1528, doi: [10.1093/mnras/stae2080](https://doi.org/10.1093/mnras/stae2080)
- Murase, K., Ahlers, M., & Lacki, B. C. 2013, *Phys. Rev. D*, 88, 121301, doi: [10.1103/PhysRevD.88.121301](https://doi.org/10.1103/PhysRevD.88.121301)
- Murase, K., Inoue, Y., & Dermer, C. D. 2014, *Phys. Rev. D*, 90, 023007, doi: [10.1103/PhysRevD.90.023007](https://doi.org/10.1103/PhysRevD.90.023007)
- Murase, K., & Ioka, K. 2013, *Phys. Rev. Lett.*, 111, 121102, doi: [10.1103/PhysRevLett.111.121102](https://doi.org/10.1103/PhysRevLett.111.121102)
- Murase, K., Kimura, S. S., Zhang, B. T., Oikonomou, F., & Petropoulou, M. 2020, *Astrophys. J.*, 902, 108, doi: [10.3847/1538-4357/abb3c0](https://doi.org/10.3847/1538-4357/abb3c0)
- Murase, K., Thompson, T. A., Lacki, B. C., & Beacom, J. F. 2011, *Phys. Rev. D*, 84, 043003, doi: [10.1103/PhysRevD.84.043003](https://doi.org/10.1103/PhysRevD.84.043003)
- NASA/IPAC Extragalactic Database (NED). 2019, NASA/IPAC Extragalactic Database (NED), IPAC, doi: [10.26132/NED1](https://doi.org/10.26132/NED1)
- NEOWISE Team. 2020, NEOWISE-R Single Exposure (L1b) Source Table, IPAC, doi: [10.26131/IRSA144](https://doi.org/10.26131/IRSA144)
- Ng, K. C. Y., & Beacom, J. F. 2014, *Phys. Rev. D*, 90, 065035, doi: [10.1103/PhysRevD.90.065035](https://doi.org/10.1103/PhysRevD.90.065035)
- Perley, D. A., et al. 2020, *Astrophys. J.*, 904, 35, doi: [10.3847/1538-4357/abbd98](https://doi.org/10.3847/1538-4357/abbd98)
- Plavin, A., Kovalev, Y. Y., Kovalev, Y. A., & Troitsky, S. 2020, *Astrophys. J.*, 894, 101, doi: [10.3847/1538-4357/ab86bd](https://doi.org/10.3847/1538-4357/ab86bd)
- Plestid, R., & Zhou, B. 2024, <https://arxiv.org/abs/2403.07984>
- Rees, M. J. 1988, *Nature*, 333, 523, doi: [10.1038/333523a0](https://doi.org/10.1038/333523a0)
- Reusch, S., et al. 2022, *Phys. Rev. Lett.*, 128, 221101, doi: [10.1103/PhysRevLett.128.221101](https://doi.org/10.1103/PhysRevLett.128.221101)
- Senno, N., Murase, K., & Meszaros, P. 2017, *Astrophys. J.*, 838, 3, doi: [10.3847/1538-4357/aa6344](https://doi.org/10.3847/1538-4357/aa6344)
- Stein, R., van Velzen, S., Kowalski, M., et al. 2021, *Nature Astronomy*, 5, 510, doi: [10.1038/s41550-020-01295-8](https://doi.org/10.1038/s41550-020-01295-8)
- Sudoh, T., Totani, T., & Kawanaka, N. 2018, *Publ. Astron. Soc. Jap.*, 70, Publications of the Astronomical Society of Japan, Volume 70, Issue 3, 1 June 2018, 49, <https://doi.org/10.1093/pasj/psy039>, doi: [10.1093/pasj/psy039](https://doi.org/10.1093/pasj/psy039)
- Tamborra, I., Ando, S., & Murase, K. 2014, *JCAP*, 09, 043, doi: [10.1088/1475-7516/2014/09/043](https://doi.org/10.1088/1475-7516/2014/09/043)
- Trakhtenbrot, B., et al. 2019, *Nature Astron.*, 3, 242, doi: [10.1038/s41550-018-0661-3](https://doi.org/10.1038/s41550-018-0661-3)
- van Velzen, S., et al. 2024, *Mon. Not. Roy. Astron. Soc.*, 529, 2559, doi: [10.1093/mnras/stae610](https://doi.org/10.1093/mnras/stae610)
- Veres, P. M., et al. 2024, <https://arxiv.org/abs/2408.17419>
- Wang, X.-Y., & Liu, R.-Y. 2016, *Phys. Rev. D*, 93, 083005, doi: [10.1103/PhysRevD.93.083005](https://doi.org/10.1103/PhysRevD.93.083005)
- Wang, X.-Y., Liu, R.-Y., Dai, Z.-G., & Cheng, K. S. 2011, *Phys. Rev. D*, 84, 081301, doi: [10.1103/PhysRevD.84.081301](https://doi.org/10.1103/PhysRevD.84.081301)
- Winter, W., & Lunardini, C. 2021, *Nature Astron.*, 5, 472, doi: [10.1038/s41550-021-01343-x](https://doi.org/10.1038/s41550-021-01343-x)
- . 2023, *Astrophys. J.*, 948, 42, doi: [10.3847/1538-4357/acbe9e](https://doi.org/10.3847/1538-4357/acbe9e)
- Wright, E. L., Eisenhardt, P. R. M., Mainzer, A. K., et al. 2010, *AJ*, 140, 1868, doi: [10.1088/0004-6256/140/6/1868](https://doi.org/10.1088/0004-6256/140/6/1868)
- Wu, H.-J., Mou, G., Wang, K., Wang, W., & Li, Z. 2022, *Mon. Not. Roy. Astron. Soc.*, 514, 4406, doi: [10.1093/mnras/stac1621](https://doi.org/10.1093/mnras/stac1621)
- Yuan, C., Winter, W., & Lunardini, C. 2024, *Astrophys. J.*, 969, 136, doi: [10.3847/1538-4357/ad50a9](https://doi.org/10.3847/1538-4357/ad50a9)

Zhou, B., & Beacom, J. F. 2020a, Phys. Rev. D, 101, 036011, doi: [10.1103/PhysRevD.101.036011](https://doi.org/10.1103/PhysRevD.101.036011)
—. 2020b, Phys. Rev. D, 101, 036010, doi: [10.1103/PhysRevD.101.036010](https://doi.org/10.1103/PhysRevD.101.036010)

—. 2022, Phys. Rev. D, 105, 093005, doi: [10.1103/PhysRevD.105.093005](https://doi.org/10.1103/PhysRevD.105.093005)